European Conference on Optical Communication (ECOC) 2022 © Optica Publishing Group 2022

Over 40-dB Link Budget, Burst-mode Digital Coherent Detection of Single Wavelength 50-Gbps Multilevel-CPFSK Signals Generated by EA-DFB-LD based Transmitter

Ryo Koma, Kazutaka Hara, Takuya Kanai, Jun-ichi Kani, and Tomoaki Yoshida

NTT Access Network Service Systems Laboratories, NTT Corporation, ryou.koma.hf@hco.ntt.co.jp

Abstract *This paper evaluates the link budget of single wavelength 50-Gbps 4-level CPFSK signals generated by simple EA-DFB-SOA based transmitter in digital coherent reception based optical access networks. We demonstrate world's first high link budget detection of over 40-dB. ©2022 The Author(s)*

Introduction

High-speed optical access networks are essential to support newly emerging bandwidth-hungry network services such as 8K video streaming, cloud-based real-time image processing, and remote operation [1-3]. Beyond-50G single-wavelength time division multiplexing based passive optical networks (TDM-PONs) have been discussed to accommodate mass-users cost effectively. Several studies have begun tackling to provide sufficient link budget including upstream burst-mode transmission of TDM PONs [4,5]. The use of optical pre/post-amplification is mandatory in high-speed PONs to achieve the standardized link budget. N1 class budget of 29 dB has been achieved by using cost-effective semiconductor optical amplifiers (SOAs) in a real-time demonstration [4]. E2 class budget of 35 dB is still challenging unless high power optical fiber amplifiers are used not only in the optical line terminal (OLT) shared by many users, but also in optical network units (ONU) due to the sensitivity limitations of direct detection (DD) [5]. This is likely to preclude cost-effective ONUs.

The application of multilevel optical phase modulation (PM) and digital coherent reception for upstream transmission provides high receiver sensitivity with electrical/optical bandwidth limited cost-effective transmitters (Txs). One key issue is to simplify the configuration of the PM-signal Tx in ONU. The use of continuous phase and frequency shift keying (CPFSK) signals is attractive because they can be generated using laser transient and adiabatic chirp by direct modulation of a distributed feedback laser diode (DFB-LD).

The digital coherent reception of CPFSK signals has been investigated for metro networks. In ref. [6], the optical signal to noise ratio characteristics after 1600-km SMF transmission were investigated with a frequency domain chromatic dispersion compensation (FD-CDC) block and a maximum likelihood sequence estimation (MLSE) in the digital signal processor (DSP) for dual polarization 25Gbaud 4-level CPFSK signals. Although the report well confirms the feasibility of the CPFSK signal transmission, some technical concerns remain with its application to upstream transmission in TDM-PONs. First, simplification of DSP blocks is desired. The conventional configuration utilizes complex angle-based processing to obtain PM signals from FSK signals and compensate chirp characteristic. Second, the residual IM component generated by injection current modulation of DFB-LD may degrade the signal to noise ratio (SNR). Third, link budget evaluations and burst-mode experiments have yet to be performed.

We have already proposed a burst-mode CPFSK Tx that combines a directly modulated (DM) DFB-LD, an electro absorption (EA) modulator, and an SOA [7]. The main advance is suppression of the residual IM component by using inverted data to drive the EA. We have also evaluated link budgets for continuous-mode 2-level 10 Gbaud CPFSK signal detection using simple DSP consisting of a delay detection block to convert the FSK signals and a linear finite impulse response (FIR) filter.

In this paper, we conduct the world's first demonstration of single wavelength 50 Gbps CPFSK signal detection with a link budget of at least 40 dB for both continuous/burst-mode signals generated by a simple EA-DFB-LD based Tx which is commonly used in conventional PONs. In addition, we experimentally investigate impact of timing and modulation amplitude mismatch between the DM-DFB-LD and the EA to the BER characteristics in the proposed Tx.

Configurations of cost-effective CPFSK Tx

Fig. 1(a) shows a single polarization CPFSK Tx consisting of a DM DFB-LD. CPFSK signals are generated by direct modulation of the injection currents of the DFB-LD [6]. The configuration is simple but offers high output power. These are great merits for an ONU Tx. However, the

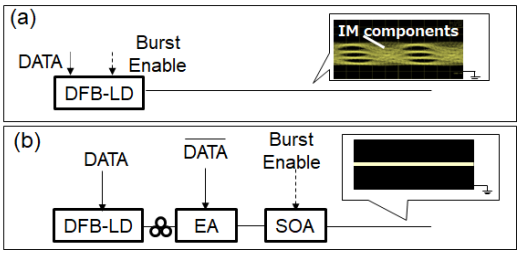

Fig. 1: Transmitter configuration based on (a) a DM-DFB-LD and (b) EA-DFB-LD integrated with booster SOA.

demerits of the configuration are as follows. First, unwanted IM components degrade the SNR because the lowest symbols have relatively low optical powers. Next, the large level DC bias modulation needed to generate burst frames yields center frequency drift to the order of several 10 GHz. This requires additional margin in the transient time or an LD driver that can suppress the drift [8].

Fig. 1(b) shows the proposed CPFSK Tx [7]; it consists of a DFB-LD, an EA modulator which suppresses IM components, and an SOA that works as not only booster but also a burst frame modulator. The configuration avoids the frequency drift since the SOA merely works as an optical shutter. Although the configuration is slightly more complicated than the former one, monolithic integration of the EA-DFB-LD and the SOA can be easily realized thanks to recent advances in monolithic integration technology [9]. We investigated the configuration shown in Fig. 1(b) in the following experiments.

Experimental setups

To evaluate the link budget of the proposal, we conducted bit error rate (BER) measurements for 50 Gbps (25-Gbaud 4-level CPFSK) signals. Fig. 2(a) shows the experimental setup. The components represented by dashed lines were used only in the burst-mode experiment. At the Tx side of the ONU, a pulse pattern generator (PPG) applied 25 Gbaud PAM4 signals with pseudo random bit sequence (PRBS) pattern of 2^7-1 to the 10G-class DM DFB-LD and the 40G-class EA. Here, low-bandwidth SMA cables were used for the EA modulator to emulate 10G-class components and 4-tap feed forward equalizers (FFEs) were utilized in the PPG to compensate the insufficient electrical bandwidth of the DFB-LD and the EA modulator . The output power and wavelength of the Tx in both continuous-mode and burst-mode experiments were 6.2 dBm and 1553.62 nm, respectively. The receiver side of the OLT included an erbium-doped fiber amplifier (EDFA) with noise figure of 4.9 dB, a DFB-LD as a Local oscillator (LO) with output power of 10 dBm, and a standard polarization diversity coherent receiver. Received signals were sampled by a digital storage oscilloscope at the sampling rate of 100 GSa/s and processed by the offline-DSP. The oversampling ratio was 4. Here, the state of polarization was set to the main axis of the coherent receiver. The wavelength difference between received signals and the LO output was set to less than 20 MHz.

The DSP for continuous-mode signal detection consisted of a 3-sample delay detection block for 4-oversample signals, carrier frequency offset compensation (CFOC) based on the vector summation method of ref. [10], a DD-LMS based 31-tap FIR filter, and an Mth power algorithm based phase compensator and a decoder. The delay detection block was utilized in order to convert FSK signals into PM signals due to its simple configuration. Fig. 2(b) shows a constellation image of obtained at the delay detection and FIR filter outputs. The constellation after differential detection shifts on the circumference of the IQ plane according to the amount of frequency transition (see Fig.2 (b) left-side as shown in Fig. 2 (a) “A”).The target values of the DD-LMS were set to each symbol position, ((1,1),(-1,1),(-1,-1),(1,-1)), represented by the red points in Fig.2 (b) right-side constellations. Assuming the application of the FIR filter coefficients handover method [11], pre-calculated coefficients were used to reduce the convergence time of the FIR filter.

For the burst-signals detection, a simple frame detection block that comparing calculated signal IQ plane radius to the threshold examined in ref. [12] and a sampling timing recovery block were added. The sampling timing recovery block played a key role in applying the FIR filter coefficients handover method by removing sampling phase differences between each burst

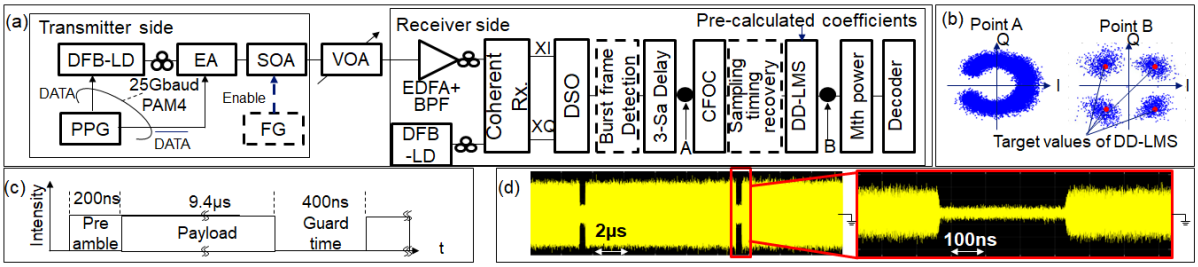

Fig. 2: (a) Experimental setup and an overview of DSP blocks using simple delay detection and DD-LMS based adaptive equalizer. (b) Received constellation images obtained at point A and point B. (c) Burst frame structure.

signal. The update interval of DD-LMS was set to 1.25 GHz assume ASIC Implementation. Fig. 2(c) and Fig.2 (d) show the burst-frame configuration and obtained signal traces at the In-phase port. Each burst frame contained a preamble of 200 ns and payload of 9.4 µs. The guard time (GT) separating the burst signals was 400 ns. A single Tx was used in the experiment because several works have well confirmed that the power difference between burst-by-burst can be compensated by automatic gain controlling of the optical amplifier or LO power adjustment [11-13].

Experimental Results

First, we evaluated the impact of modulation amplitude and timing mismatch between the DM-DFB-LD and the EA modulator to the BER characteristics. Fig. 3(a) shows the output signal images in the case of modulation amplitude mismatch. Here, we defined peak to peak power difference of the residual IM component as ΔP. Fig. 4 plots BER characteristics against ΔP at the input power of -30 dBm for continuous-mode signals. As shown in the figure, BER degrades as ΔP increases. The IM components could not be completely removed due to the difference in frequency characteristics. The minimum ΔP was 0.7 dB (see the obtained eye pattern in the inset of Fig. 4). The results also represent the effect of IM components suppression. Another factor as regards to degradation of signal quality is modulation timing error. Fig. 3(b) shows the output signal images. In such cases, severe overshoots happen at the edge of each bit. Fig.5 (a) plots the measured ΔP against timing error of ΔT controlled by the changing delay value of the PPG. Fig. 5(b) shows obtained BERs. As shown in the figure, the minimum BER was obtained at ΔT = -10 ps, where the EA modulation precedes DFB-LD modulation. We assume that was caused by interaction between chirp characteristics of the DM-DFB-LD, the EA modulator and the SOA.

Fig. 6 plots measured BERs against received signal powers for the case of ΔP =0.7 dB and ΔT =-10 ps. Here, the receiver sensitivity defined at the received signal power of BER=10^{-2} assuming the use of low-density parity check coded forward error correction (LDPC-FEC). The receiver sensitivities for continuous-mode and burst-mode signals were -35.0 dBm and -34.5 dBm, respectively. According to the results, an error floor observed for burst-mode signals even though the obtained BERs were less than the FEC limit. The sensitivity penalty with continuous-mode detection was 0.5 dB. We assume that the BER degradation was caused by insufficient convergence of FIR filter coefficients since the optimal value of the coefficient varies against the residual CFO, the sampling phase, and so on. Nevertheless, the much high link budget of 40.7 dB was achieved even in the case of burst-mode signal detection. The obtained budgets not only provide the E2 class link budget of 35 dB but also enhancement of PON splitting ratio and reach.

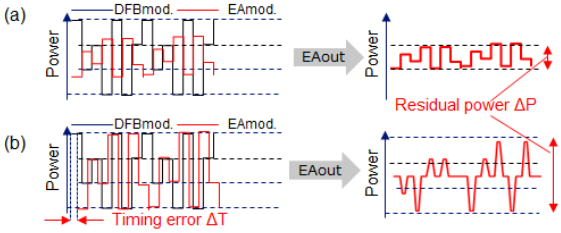

Fig. 3: Output signal images for (a) modulation power and (b) timing errors between the DFB-LD and the EA.

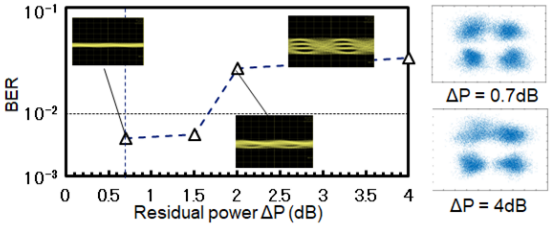

Fig. 4: BER characteristics against residual power and obtained constellations at input power of -30 dBm.

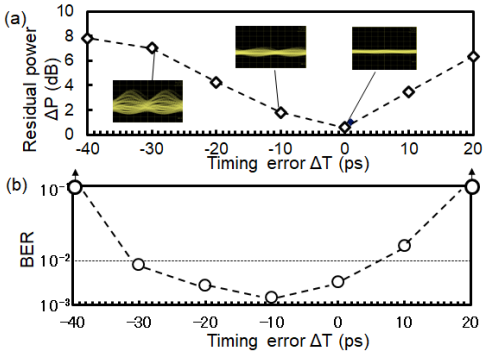

Fig. 5: (a) Characteristics of residual IM component and (b) BER against timing errors at the input power of -30 dBm.

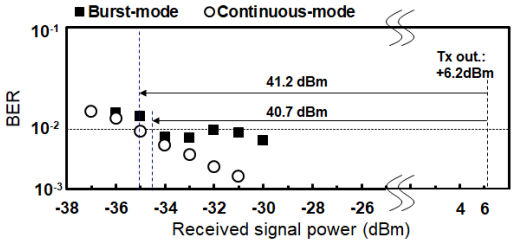

Fig. 6: BER characteristics

Conclusions

We experimentally demonstrated 50-Gbps 4-level CPFSK continuous-mode and burst-mode signal digital coherent detection with the extremely high link budgets of 41.2 dB and 40.7 dB, respectively. We consider that a simple SOA monolithically integrated EA-DFB-LDs is viable for realizing beyond 50G-class ONUs in a cost effective manner.

References

[1] E. Harstead, D. van Veen, V. Houtsma and P. Dom, "Technology Roadmap for Time-Division Multiplexed Passive Optical Networks (TDM PONs)," in Journal of Lightwave Technology, vol. 37, no. 2, pp. 657-664, 15 Jan.15, 2019, DOI: 10.1109/JLT.2018.2881933.

[2] H. Kawahara, T. Seki, S. Suda, M. Nakagawa, H. Maeda, Y. Mochida, Y. Tsukishima, D. Shirai, T. Yamaguchi, M. Ishizuka, Y. Kaneko, K. Koshiji, K. Honda, T. Kanai, K. Hara and S. Kaneko ., "Optical Full-mesh Network Technologies Supporting the All-Photonics Network Visual System-response Functions and Estimating Reflectance," NTT Technical Review, Vol. 18 No. 5,May 2020, pp. 24-29.

[3] D. Welch, A. Napoli, J. Bäck, W. Sande, J. Pedro, F. Masoud, C. Fludger, T. Duthel, H. Sun, Steven J. Hand, T.-K. Chiang, A. Chase, A. Mathur, T. A. Eriksson, M. Plantare, M. Olson, S. Voll, and K.-T. Wu, "Point-to-Multipoint Optical Networks Using Coherent Digital Subcarriers," J. Lightwave Technol. 39, 5232-5247 (2021), Doi: 10.1109/JLT.2021.3097163.

[4] G. Simon, F. Saliou, J. Potet, P. Chanclou, R. Rosales, I. N. Cano, and D. Nesset, "50Gb/s Real-Time Transmissions with Upstream Burst-Mode for 50G-PON using a Common SOA Pre-amplifier/Booster at the OLT," 2022 Optical Fiber Communications Conference and Exhibition (OFC), 2022, pp. 1-3, DOI: 10.1364/OFC.2022.M3G.3

[5] H. Chen, N. K. Fontaine, M. Mazur, L. Dallachiesa, Y. Zhang, H. Huang, D. van Veen, V. Houtsma, A. Blanco-Redondo, R. Ryf, D. T. Neilson, "140G/70G Direct Detection PON with >37 dB Power Budget and 40-km Reach Enabled by Colorless Phase Retrieval Full Field Recovery," 2021 European Conference on Optical Communication (ECOC), 2021, pp. 1-4, DOI: 10.1109/ECOC52684.2021.9605860.

[6] Di Che, Feng Yuan, and William Shieh, "Maximum likelihood sequence estimation for optical complex direct modulation," Opt. Express 25, 8730-8738 (2017) DOI:10.1364/OE.25.008730

[7] M. Fujiwara, R. Koma, J. Kani, K. Suzuki, and A. Otaka, "Performance Evaluation of CPFSK Transmitters for TDM-Based Digital Coherent PON Upstream," in Optical Fiber Communication Conference, OSA Technical Digest (online) (Optica Publishing Group, 2017), paper Th1K.5, DOI:10.1364/OFC.2017.Th1K.5

[8] H. Debrégeas, R. Borkowski, R. Bonk, R. Brenot, J.-G. Provost, S. Barbet, and T. Pfeiffer, "TWDM-PON Burst Mode Lasers With Reduced Thermal Frequency Shift," in Journal of Lightwave Technology, vol. 36, no. 1, pp. 128-134, 1 Jan.1, 2018,DOI: 10.1109/JLT.2017.2753281.

[9] M. Chen, T. Shindo, S. Kanazawa, Y. Nakanishi, A. Kanda, T. Yoshimatsu, and K. Sano, "High-power SOA-integrated EADFB laser for long-reach passive optical network systems," OSA Continuum 4, 498-506 (2021) DOI: 10.1364/OSAC.411423

[10] T. Kanai, R. Koma, M. Fujiwara, R. Igarashi, N. Iiyama, J.-I. Kani, A. Otaka, "Wide-Range Frequency Offset Compensation for CPFSK Used as TOM-Based Digital Coherent PON's Upstream Signals," 2018 European Conference on Optical Communication (ECOC), 2018, pp. 1-3, DOI: 10.1109/ECOC.2018.8535224.

[11] R. Koma, M. Fujiwara, J. Kani, K. Suzuki and A. Otaka, "Burst-mode digital signal processing that pre-calculates FIR filter coefficients for digital coherent pon upstream," in Journal of Optical Communications and Networking, vol. 10, no. 5, pp. 461-470, May 2018, DOI: 10.1364/JOCN.10.000461.

[12] R. Koma, M. Fujiwara, J.-I. Kani, S.-Y. Kim, T. Suzuki, K.-I. Suzuki, and A. Otaka, "Demonstration of Real-Time Burst-Mode Digital Coherent Reception With Wide Dynamic Range in DSP-Based PON Upstream," in Journal of Lightwave Technology, vol. 35, no. 8, pp. 1392-1398, 15 April15, 2017, DOI:10.1109/JLT.2016.2637357.

[13] G. Li, S. Xing, Z. Li, J. Zhang, and N. Chi, "200-Gb/s/λ Coherent TDM-PON with Wide Dynamic Range of >30-dB based on Local Oscillator Power Adjustment," in Optical Fiber Communication Conference (OFC) 2022, S. Matsuo, D. Plant, J. Shan Wey, C. Fludger, R. Ryf, and D. Simeonidou, eds., Technical Digest Series (Optica Publishing Group, 2022), paper Th3E.3, DOI: 10.1364/OFC.2022.Th3E.3.